Published in final edited form as:
Cell. 2014 January 30; 156(3): 549–562. doi:10.1016/j.cell.2013.12.025.

Progesterone Receptor in the Vascular Endothelium Triggers Physiological Uterine Permeability Pre-implantation

Lauren M. Goddard[1], **Thomas J. Murphy**[2], **Tönis Org**[1], **Josephine M. Enciso**[3], **Minako K. Hashimoto-Partyka**[1], **Carmen M. Warren**[1], **Courtney K. Domigan**[1], **Austin McDonald**[2], **Huanhuan He**[4], **Lauren A. Sanchez**[1], **Nancy C. Allen**[1], **Fabrizio Orsenigo**[6], **Lily C. Chao**[5], **Elisabetta Dejana**[6], **Peter Tontonoz**[5], **Hanna K.A. Mikkola**[1,2], and **M. Luisa Iruela-Arispe**[1,2,*]

[1]Department of Molecular, Cell and Developmental Biology, University of California, Los Angeles, Los Angeles, CA 90095, USA

[2]Molecular Biology Institute, University of California, Los Angeles, Los Angeles, CA 90095, USA

[3]Division of Neonatology, Department of Pediatrics, University of California, Los Angeles, Los Angeles, CA 90095, USA

[4]Department of Human Genetics, University of California, Los Angeles, Los Angeles, CA 90095, USA

[5]Department of Pathology, University of California, Los Angeles, Los Angeles, CA 90095, USA

[6]IFOM, Foundation FIRC Institute of Molecular Oncology, 20139 Milan, Italy

Summary

Vascular permeability is frequently associated with inflammation and triggered by a cohort of secreted permeability factors such as VEGF. Here we show that the physiological vascular permeability that precedes implantation is directly controlled by progesterone receptor (PR) and is independent of VEGF. Both global and endothelial-specific deletion of PR block physiological vascular permeability in the uterus whereas misexpression of PR in the endothelium of other organs results in ectopic vascular leakage. Integration of an endothelial genome-wide transcriptional profile with ChIP-sequencing revealed that PR induces a NR4A1 (Nur77/TR3)-dependent transcriptional program that broadly regulates vascular permeability in response to progesterone. Silencing of NR4A1 blocks PR-mediated permeability responses indicating a direct link between PR and NR4A1. This program triggers concurrent suppression of several junctional proteins and leads to an effective, timely and venous-specific regulation of vascular barrier function that is critical to embryo implantation.

Introduction

The endothelium constitutes a highly specialized cell population that lines the inner layer of the vascular tree. The particular location of blood vessels imposes functional demands,

*Please address correspondence to: Luisa Iruela-Arispe, Ph.D., Terasaki Life Sciences Building, 610 Charles E. Young Drive East, Los Angeles, CA 90095-7239, arispe@mcdb.ucla.edu, Phone: 310-794-5763, Fax: 310-794-5766.

The authors have no conflicting financial interest.

intrinsic to each organ, that exceed its well-accepted role as a barrier and non-thrombogenic surface. To accommodate organ-specific functions, endothelial cells differ in regard to structure, adhesion molecules, metabolic properties, antigenic expression and cell surface determinants (Atkins et al., 2011; Chappell and Bautch, 2010; Regan and Aird, 2012). However, we are significantly behind in our understanding of how unique vascular functions are developed and maintained to offer specific properties to individual tissues.

In the endometrium, cycles of vascular repair and angiogenesis are additional to the underlying organ-specific requirements. The repair and re-growth of the endometrium is driven by the sequential and tightly controlled interplay of steroid hormones. In particular, endometrial angiogenesis appears to be regulated by 17-β estradiol (E2), likely through the ER-β receptor as per its high expression in the primate endometrial vascular and perivascular cells (Arnal et al., 2010; Kim and Bender, 2009). Consistent with this prediction, low concentrations of E2 induce proliferative and migratory responses in endothelial cells (Bernelot Moens et al., 2012). More importantly, ER-β knockout mice acquire abnormal vascular function and hypertension associated with endothelial dysfunction and impaired angiogenesis (Iafrati et al., 1997; Zhu et al., 2002). Furthermore, E2 regulates expression of VEGF and has been shown to promote vascular expansion in the endometrium of primates (Hyder et al., 1996; Sugino et al., 2002).

A second unique feature of endometrial vessels is cyclic alterations in vascular permeability. These events result in the recurrent formation of a physiological edema during the second half of the endometrial cycle (secretory phase), a time when progesterone (P4) levels peak (Strauss and Barbieri, 2009). Increased permeability alters the functional endometrium and makes it receptive for embryonic implantation. As part of the decidual response, changes in the degree of permeability parallel the ovarian cycle and are extremely pronounced during pregnancy (Gellersen et al., 2007). The leakage of blood-borne proteins to the interstitium is critical to support the highly metabolic trophoblastic cells and to the survival of the blastocyst. Interestingly, animals that lack PR are unable to mount a decidual response (Lydon et al., 1996; 1995), placing PR as the upstream coordinator of the cellular and molecular changes that regulate decidualization, including alterations in the stroma, matrix and vasculature (Large and DeMayo, 2012).

In this study, we provide evidence that PR is required within the endothelial compartment to mediate physiological vascular permeability. The resulting edema is independent of VEGF and instead triggered by PR-dependent activation of nuclear receptor subfamily, group A, member 1 (NR4A1). Ultimately, through this mechanism, PR is able to selectively target the endometrial vasculature in a coordinated and sustained permeability response.

Results

Complete Deletion of PR Leads to Reduced Physiological Vascular Permeability

To dissect the biological function of PR in the endometrial vasculature, we first examined mice with global deletion of PR (PRKO) and littermate controls. Exposure of control mice to P4 resulted in uterine hyperplasia (Figure 1A) with a concurrent weight increase of 2.5-fold (Figure 1F). In contrast, PRKO uteri failed to mount an equally significant response (Figure 1A,F). Sections stained with a collagen IV antibody or perfused intravascularly with *Lycopersicon esculentum* lectin showed equivalent vascular density between groups whether treated with vehicle or hormones (Figure 1B,C,D). Histological analysis also revealed similar overall structure between control and PRKO mice (Figure S1A), however expression of mucin1, an epithelial glycoprotein, and several proteoglycans, were decreased in PRKO uteri (Figure S1B). These differences were indicative of deficiencies in the differentiation of the uterus.

As uterine hyperplasia could be due to increased interstitial fluid, we assessed whether the changes in uterine weight were due to an accumulation of plasma proteins extravasated from the vascular compartment. Hormone (E2 and P4) treatment of control mice resulted in a 3.8-fold increase in Evans blue content. This was in contrast to PRKO mice that showed no differences in uterine permeability (Figure 1G). Furthermore, inhibition of PR by mifepristone (RU486) blocked the effect of P4 on uterine weight (Figure 1H) and Evans blue extravasation (Figure 1I), while inhibitors of other permeability mediators: VEGFR2 (SU11248) and bradykinin (HOE 140) had no effect. These results suggest that P4, through PR, regulates uterine vascular permeability independent of classical pathological permeability mediators.

PR Expression in the Vasculature is Restricted to Endothelial Cells of Veins and Lymphatics of the Uterus and Ovary

As the endothelium is largely responsible for regulation of vascular permeability, we first evaluated whether the effect of P4 on barrier function was direct, and through PR expression in endothelial cells. Presence of PR in the vasculature has been a point of debate with a number of publications supporting (Krikun et al., 2005; Maybin and Duncan, 2004; Vázquez et al., 1999) and negating expression in endothelial and smooth muscle cells (Ismail et al., 2002; Perrot-Applanat et al., 1995). Using PRLacZ mice (Figure S2), which report both PRA and PRB promoter activation, we found that indeed endothelial cells were β-gal positive (Figure 2A). Interestingly, PR positive endothelial cells were restricted to venules and lymphatics of the uterus and ovary, but absent from arterioles (Figure 2A, S2G). Smooth muscle cells and/or pericytes were also positive, however β-gal reactivity was equivalent in both arterioles and venules (Figure 2A). Under physiological conditions, PR promoter activity was not detected in the vascular beds of any other organs (Figure S2H) revealing an exclusive organ-specificity for PR to vessels of the uterus and ovary.

Expression of PR in the vasculature was confirmed at the protein level by immunohistochemistry. Similar to findings from PRLacZ reporter mice, endothelial cells of veins and lymphatic vessels were positive for both PECAM-1 and PR, while arterial endothelial cells lacked PR expression (Figure 2B). Expression of PR in human endometrium was also exclusive to the endothelium of veins (Figure 2C).

It should be emphasized that PR expression in the endothelium is not constitutive. On average, at any given time PR positive endothelial cells represent 22.7% (32.5% following hormone treatment) of uterine venous and 21% of lymphatic (24% following hormone treatment) endothelial cells per vessel cross section (Figure 2D). Additionally, on average 30%–40% of uterine vessels express at least one β-gal+ endothelial cell (Figure 2E). Upon pregnancy, transcripts for PR increase by 4.5 fold in the uterus (Figure 2F) and by 3.2 fold in FACS sorted endothelial cells (Figure 2G). Furthermore, the frequency of PR+ endothelial cells is also increased specifically in veins at day 5.5 of gestation (Figure 2H,I).

PR Signaling in the Endothelium Promotes Vascular Permeability in vivo

To determine whether the effect in vascular permeability was due to PR activity in endothelial cells, we evaluated cell-specific deletion of PR (PR^{ECKO} mice) (Figure S3A,B). Cre expression in the uterus and ovary is completely restricted to the endothelium of the vasculature as determined by β-gal positivity using R26R reporter mice (Figure S3C). The effect of recombination was highly penetrant as demonstrated by PR deletion in FACS sorted endothelial cells (Figure S2E,F).

Using the Miles assay, control and PR^{ECKO} mice were examined for changes in permeability following hormone treatment (E2+P4). PR^{ECKO} uteri had significantly reduced

Evans blue content, yet the duodenum, which lacks PR expression, did not exhibit changes in permeability (Figure 3A,B). These results were confirmed by measurements of albumin in the interstitial uterine tissue (Figure 3C,D). While, hormone-treated control animals exhibited a 4.79-fold increase in albumin levels; PR^{ECKO} mice, albeit responsive, only showed a 1.9-fold increase of no statistical significance (Figure 3C). Albumin levels in PRKO mice were not affected by treatment. It should be stressed that PRKO mice showed greatly reduced levels of proteoglycans (Figure S1B), which have been shown to be important for water retention and likely contribute to explain this effect. As expected, pregnancy increased albumin extravasation in control mice, yet this effect was significantly reduced in PR^{ECKO} mice (Figure 3D).

To explore the biological relevance of these findings, we performed implantation assays in control and PR^{ECKO} mice (Figure 3E). The results revealed a 43% reduction in the number of implantation sites in PR^{ECKO} mice compared to controls (Figure 3F). Because PR has been shown to regulate VEGF, we sought to evaluate the effect of blocking VEGFR2 during pre- and post-implantation times. P4 blockade, as anticipated, prevented implantation at all gestational time points examined, whereas inhibition of VEGF signaling only impacted embryo viability when administered at post- but not pre-implantation times (Figure 3G).

Absence of PR in the endothelium did not change vascular density (Figure S3D) but affected vascular function. Veins specifically failed to exhibit signs of vascular leakage as shown by injection with *Ricinus communis agglutinin I* (RCAI) lectin (Figure 3H). Phosphorylation of VE-Cadherin, a molecular read-out of barrier instability was present at the interface of PR positive cells, while PR negative cells showed reduced pVE-Cadherin (Figure 3I). This finding was also confirmed by total protein lysates from uteri of control and PR^{ECKO} mice (Figure 3J). Finally, while permeability associated with pregnancy resulted in an increase in VE-Cadherin phosphorylation, this effect was muted in PR^{ECKO} mice (Figure 3K).

The function of PR in endothelial cells was further scrutinized by ectopic expression using a transgenic mouse model (Figure S3G, Table S1). Relative levels of transgenic PR protein confirmed that the lung was by far the site of highest expression followed by the intestine, with complete absence from the kidney, uterus, and heart (Figure S3H,I,J). Consistent with lack of transgene expression in uteri, P4 treatment resulted in equivalent extravasation of Evans blue (Figure S3K). In contrast, vascular permeability in PRTg lungs was 5.3-fold greater than baseline, while leakage in the duodenum increased by 1.6 fold (Figure S3L,M). Immunohistochemical analysis of RCAI-injected mice revealed barrier dysfunction in the lung following hormone treatment and provided additional support to the Miles assay (Figure S3N).

PR Activation in Endothelial Cells Results in Inter-endothelial Gaps and Decreased Endothelial Monolayer Resistance

Having established that endothelial PR promoted vascular permeability in vivo, we returned to in vitro settings to gain mechanistic insights. First we examined human endometrial endothelial cells (HEEC) that express endogenous PR. Similar to the findings in the murine and human endometrial sections, presence of PR was heterogeneous (Figure 4A), an important advantage as it allowed for concurrent assessment of PR negative cells in the same culture. To determine the effect of P4 on junctional complexes, we used β-catenin immunolocalization. Cell-cell integrity was stable in non-treated (Figure 4a) and vehicle treated HEECs (Figure 4b). However, P4 treatment induced translocation of β-catenin away from adherens junctions and resulted in the formation of intercellular gaps only in HEECs expressing PR (orange nuclei), while cells that lacked PR remained bound (Figure 4c, bracket).

A more comprehensive evaluation of the effect of PR on junctional proteins was performed in umbilical vein endothelial cells (HUVECs) infected with a PR lentivirus (Figure 4B,C). Exposure to P4 resulted in clear loss of PECAM-1 (Figure 4B), VE-Cadherin (FigureS4A) and β-catenin cell surface expression (Figure 4C). Biochemically β-catenin was found to translocate from the cell membrane to the cytosol and nucleus upon treatment with P4 (Figure 4C,D). These effects were absent in HUVECs that lack PR whether in the presence or absence of P4 (Figure S4B).

To evaluate the progression of junctional breakdown in real-time, we used Electrical Cell-Substrate Impedance Sensing (ECIS) on endothelial monolayers (Figure 4E). Following P4 treatment, human dermal endothelial cells (HDECs) overexpressing PR exhibited a progressive decrease in resistance, with initial barrier destabilization occurring between 4–8h after P4 addition (Figure 4F). At 17h, the reduction in barrier resistance was equivalent to that induced by thrombin (at 30 min), a landmark control for these types of experiments. Notably, in contrast to the short effect mediated by thrombin, P4 exposure resulted in persistent and continuous barrier breakdown.

To confirm that the changes in resistance were due to cellular gaps, we visualized β-catenin expression in the same cells measured by ECIS. As expected, cells that exhibited a decrease in electrical resistance also displayed discontinuous cell-cell adhesion (Figure S4C). Furthermore, the effects on barrier integrity were found to be dose-dependent (Figure 4G) and ceased after removal of P4 (at physiological levels) (Figure 4H). Surprisingly, inhibition of classical permeability signaling molecules including Src (Figure S4D), PI3K (Figure S4E), ROCK (Figure S4G), and VEGFR2 (Figure S4H) did not inhibit P4-induced permeability, nor did taxol-mediated microtubule stabilization (Figure S4F), suggesting that a novel mechanism may act downstream of PR.

Endothelial PR Signaling Alters Junctional Protein Expression

Using next generation RNA sequencing, we explored the notion that PR signaling may transcriptionally alter the expression of endothelial junctional proteins. Following 4h of P4 treatment, we compared the fold change of several genes known to regulate vascular permeability (Figure 5A). As expected, many of the genes that encode proteins important for junctional stability such as VE-cadherin (*CDH5*), VE-PTP (*PTPRB*), PECAM-1, and claudin-5 (*CLDN5*) were reduced upon P4 exposure. qPCR analysis of VE-cadherin and Claudin-5 confirmed the reduction noted by RNA-seq (Figure 5B). Western blot analysis demonstrated significant reduction in junctional protein levels starting at 16h post-treatment (Figure 5C,D), supporting the kinetics revealed by HUVEC immunofluorescence (Figure S4A). β-catenin levels remained unchanged both at the RNA and protein level, which correlated with protein translocation rather than reduction. Other endothelial-matrix associated proteins including focal adhesion kinase (FAK) and β1-integrin were not affected by P4 addition (Figure S5A).

To determine whether transcriptional activation and subsequent protein synthesis were required for P4-mediated permeability, HUVECs were treated with inhibitors of transcription and translation (Figure 5E,F). Both inhibitors completely blocked the decrease in monolayer resistance observed upon P4 treatment, confirming the requirement for transcriptional regulation and de novo protein synthesis downstream of PR signaling.

PR Directly Binds to the NR4A1 Promoter and Regulates NR4A1 Gene Expression

A concrete elucidation of PR's mechanism of action required us to ascertain the cohort of PR-regulated genes in the endothelium and identify within this cohort the intermediate effector(s). We were led to obtain a global read-out of PR binding sites in the HUVEC

genome using chromatin immunoprecipitation (ChIP). In the absence of ligand (PR only) we resolved 525 PR binding sites, while activation of the receptor by P4 (PR+P4) resulted in a much higher number (9,906) of PR binding sites, 396 of which overlapped with PR only peaks. To identify genes that might be regulated by PR we next associated PR+P4 binding sites (9,906) with nearby genes within a 50kb range from transcriptional start sites and identified 3,886 predicted bound genes following P4 treatment (Figure 6A).

To find direct PR target genes whose expression was affected in response to P4, it was necessary to combine the ChIP-seq and RNA-seq datasets (Figure 6B). RNA-seq analysis of HUVECs yielded 406 upregulated and 431 downregulated genes with a pvalue less than 0.01 (Figure 6B). These genes were then intersected with the list of 3,886 genes predicted as regulated by the PR binding sites obtained from ChIP-seq evaluation. This analysis showed that 93 (23%) of activated and 214 (49%) of repressed genes are likely direct targets of PR in endothelium. To identify which biological processes PR might regulate, directly activated (Figure 6C) and repressed (Table S2) gene lists were subjected to the DAVID Bioinformatics Database for gene ontology (GO) (Huang et al., 2009). Interestingly, transcription was the top term associated with directly upregulated genes (Figure 6C). As P4 mediated permeability requires de novo protein synthesis, we further focused on the 28 transcription factors directly upregulated by PR by examining fold upregulation post P4 treatment (Figure 6D).

Notably, only one of these transcription factors, NR4A1, has been previously implicated in vascular permeability (Zhao et al., 2011). Two distinct PR binding peaks were found between 10–25kb upstream of the NR4A1 start site in PR+P4 samples, but not in respective controls (Figure 6E). qPCR confirmed significant NR4A1 upregulation as early as 1h after P4 addition (Figure 6F). Interestingly, NR4A1 expression continued to increase and sustained elevated levels as long as 24h after P4 stimulation. To further validate direct PR binding at the NR4A1 locus, intervals putatively containing PR binding, along with a negative control region, were analyzed by ChIP-qPCR (Figure 6G). PR binding was significantly enriched at both regions corresponding to ChIP-seq peaks, as compared to control samples (Figure 6G).

NR4A1 is Required for Progesterone Mediated Endothelial Permeability

Endothelial barrier stability was enhanced when NR4A1 was knocked-down using siRNA (Figures 7A,B). While P4 increased permeability in PR-expressing HUVECs, this effect was largely blocked by the knockdown of NR4A1 (Figure 7C). To further scrutinize these conclusions, HUVECs were infected with an adenovirus containing a dominant negative (NR4A DN) construct for all NR4A family members (Pei et al., 2006). Similar to NR4A1 knockdown, overexpression of the NR4A DN inhibited P4-mediated permeability (Figure 7D).

Immunocytochemistry further supported the concept that NR4A1 acts downstream of PR to regulate barrier breakdown in endothelial cells. Although HUVECS treated with non-targeting siRNA showed reduced VE-cadherin and PECAM-1 levels as well as β-catenin relocalization, effects were blocked in cells with NR4A1 knocked down (Figure 7E). Interestingly, knockdown of NR4A1 led to an increase in membrane expression of all three junctional proteins, consistent with the increase in basal resistance seen by ECIS. Protein analysis further demonstrated the reduction of claudin-5, PECAM-1, and VE-cadherin in HUVECs transfected with non-targeting siRNA (Figure 7F, S7A–C). PR levels between non-targeting and knockdown cells were similar, ruling out possible changes in PR expression as the determinant of this effect.

Since PR also directly stimulates NR4A2 expression (Figure S6A–C), we examined the effect of NR4A2 reduction on permeability (Figure S6D). Knockdown of NR4A2 by three independent siRNA constructs did not inhibit P4-mediated permeability, demonstrating a unique role for NR4A1 in the regulation of the endothelial barrier (Figure S6E).

In vivo expression of NR4A1 was examined using a GFP reporter mouse (Table S1). GFP, as a read-out of NR4A1, was largely restricted to the vasculature, particularly endothelial cells (Figure 7G). Unlike PR expression, NR4A1 was seen in both veins and arteries but co-localization of PR and NR4A1 was frequently found in veins (Figure 7H). Using qPCR of whole uteri, we found that NR4A1 expression is responsive to P4 stimulation as mRNA levels were 3.8-fold higher following treatment. This same increase was not seen in PR^{ECKO} mice, suggesting that PR signaling in the endothelium enhances NR4A1 expression (Figure 7I). To determine whether loss of NR4A1 had biological implications to uterine vascular permeability, we examined Evans blue extravasation following hormone stimulation in NR4A1 null mice. Similar to PR^{ECKO} mice, a significant reduction in Evans blue content was seen in the uterus of NR4A1 KO mice, but not the intestine (Figure 7J).

The ability of NR4A1 to directly control expression of junctional proteins was also tested in gain-of-function experiments. Overexpression of NR4A1 resulted in a marked reduction in VE-cadherin, claudin-5, and PECAM-1 in the absence of P4 (Figure S7E). Furthermore, expression of NR4A1 alone increased monolayer resistance as determined by ECIS (Figure S7D), providing additional functional validation. These results indicate that NR4A1 is required and acts downstream of PR to mediate endothelial specific vascular permeability.

Discussion

The sequential and highly coordinated action of the steroid hormones E2 and P4 are known to regulate epithelial and stromal functions in the endometrium (Das et al., 2009; Gellersen et al., 2007; Wetendorf and DeMayo, 2012). Changes imposed by these steroid hormones prepare the endometrium for implantation and continue to be essential during the subsequent post-implantation phases to ensure a successful pregnancy (Franco et al., 2012; Wetendorf and DeMayo, 2012). Whereas much is known about the molecular and cellular events downstream of epithelial and stromal responses, the unique series of changes imposed to the uterine vasculature prior, during and post-implantation are only known at the level of morphological description. Here we show that PR within the endothelium is responsible for initiating a series of events that lead to physiological edema in the endometrium. Specifically, PR induces expression of the orphan nuclear receptor NR4A1, which, in turn, destabilizes endothelial barrier function within PR-expressing endothelial cells. The consequence is restricted and sustained vascular permeability directed by circulating P4.

The contribution of P4 as the chief regulator of vascular alterations during the secretory phase was implied from earlier work noting that mice with lack of PR failed to mount a decidual response (Lydon et al., 1995; 1996). Because expression of PR in the endothelium was not constitutive, we believed that the effect on vessels was triggered through the secondary action of permeability modulators. An obvious culprit, VEGF, has been frequently evoked as responsible for the cycle of vascular changes in the uterus. In fact, VEGF is induced by steroid hormones (Hyder et al., 1996; Shifren et al., 1996; Sugino et al., 2002) and pharmacological blockade of this growth factor in primates impairs endothelial repair and angiogenic growth (Fan et al., 2008). Surprisingly, we found that blockade of VEGF does not prevent the physiological edema that occurs prior to implantation; instead these events appear to be triggered by P4-driven mechanisms that are independent of VEGF. These findings pointed to either alternative permeability mediators or a direct role of PR in the endothelium. It should be noted, however, that inactivation of VEGF signaling post-

implantation, like P4 blockade, impacts both permeability and embryo viability. Thus, it appears that the mechanisms that regulate permeability responses pre- and post-implantation are likely distinct.

To evaluate the contribution of PR in the vascular endothelium, we adopted loss and gain-of-function approaches. Mice that lack PR in the endothelium, albeit able to host the typical decidual response by stromal cells, showed impaired ability to mount a physiological edema response with consequences to implantation. In contrast, transgenic animals that mis-expressed PR on endothelial cells in organs other than the uterus displayed an acute permeability response upon ligand exposure. Together these findings implicated P4 as the mediator of the permeability responses in the uterus.

How does P4 drive vascular permeability? Although the molecular mechanisms of P4 action via binding to its receptor are well established (Edwards et al., 1995; McKenna and O'Malley, 2000; Rubel et al., 2012), the effects of this hormone on endothelial cells have not been explored at the molecular level. Evaluation of the literature on the effect of PR in epithelial cells was not informative as to how, in endothelial cells, this transcription factor could promote destabilization of barrier function. Furthermore, our in vitro experiments indicated that the effect of PR on endothelial permeability required transcriptional control. Following that lead, we performed global transcriptional profiling (RNA-seq) of endothelial cells treated with P4. These data initially failed to provide insights into the process whereby PR promotes permeability. It was only through the integration of ChIP-sequencing analysis with the transcriptional profile that we were able to identify NR4A1 as the possible link.

The orphan nuclear receptor NR4A1 is a member of the NR4A transcription factor family that is expressed by a broad number of cell types. The effects mediated by NR4A1 are pleotropic, cell-type dependent and impact metabolism, homeostasis and inflammation (Pearen and Muscat, 2010; Zhao and Bruemmer, 2010). Recently NR4A1 has been also shown to be expressed by endothelial cells and to induce pathological permeability responses (Zhao et al., 2011). The reports implicating NR4A1 in permeability opened the possibility for a role of NR4A1 downstream of PR signaling.

A hallmark of vascular leakage is the formation of intercellular gaps via disruption of cell-cell contacts resulting in a loss of barrier integrity (Dejana et al., 2008; Dvorak, 2010; Komarova and Malik, 2010). Along these lines, endothelial cells expressing PR showed disruption of cell-cell interactions upon exposure to the ligand. Interestingly, silencing of NR4A1 in cells expressing PR and treated with the ligand blocked the effect of P4 on permeability. These findings clearly indicated that PR was upstream of NR4A1 in the control of endothelial barrier function. Furthermore, we found that NR4A1 coordinates an effective program of repression of junctional proteins, including VE-Cadherin, Claudin-5 and PECAM1.

Our results indicate that under homeostatic conditions, PR is highly restricted to uterine blood vessels, at the exclusion of vessels from other organs. Interestingly, expression of PR is selective to veins and lymphatic vessels. Endothelium from arteries is conspicuously absent of PR, while expression is highly noted in the smooth muscle layer of these vessels. This exquisite specificity enables local and controlled functions triggered by a systemically distributed ligand.

Is PR the only regulator of permeability in the uterus? Unlikely, but our findings would indicate that removal of this receptor from the endothelium significantly impacts permeability and implantation. This is in sharp contrast to VEGF blockade for example, which did not impact embryo viability at pre-implantation times. Another important point, genomic inactivation of PR completely blocks permeability. Initially, this finding led us to

imply that PR might regulate permeability through its actions in other cell types. However, comparisons between global and cell-specific PR are confounded by the global impact of PR in the differentiation of the uterus. In fact, deletion of PR from the onset of development impacts the differentiation of uterine epithelium and stroma, including reduction in proteoglycan levels (Figure S1B) that are critical to interstitial water retention and contribute to regulation of fluid trafficking in tissues. This might explain why PRKO mice exhibit a much lower basal content of albumin, while control and PR^{ECKO} mice are equivalent at baseline and only differ upon hormonal treatment.

The findings presented here are in accordance with, and further explain, the uterine vascular fragility experienced by users of long-term progestin-only contraceptives (Hickey and Fraser, 2002; Kovacs, 1996; Shoupe et al., 1991). In fact, prolonged exposure to progestins results in abnormal endometrial bleeding despite increased levels of tissue factor expression (Runic et al., 2000).

Structural and molecular differences in the endothelium of distinct tissues reflect its role in meeting the diverse requirements of individual organ sites. The recurrent cycles of physiological permeability in the endometrium are unique to this tissue and must be timely regulated. Here we showed that this physiological permeability requires a molecular toolkit distinct from that of pathological permeability. Combined the findings highlight the process by which endothelial cells detect and respond to systemic hormones to trigger local, timely and effective changes in barrier function.

Experimental Procedures

Mouse Models

Details about mouse models and genotyping can be found in Extended Experimental Procedures. All animals were housed in a pathogen-free environment in an AAALAC-approved vivarium at UCLA, and experiments were performed in accordance with the guidelines of the Committee for Animal Research.

Hormone Treatment

8–12 week old female tie1-PRTg, PRLacZ, PR^{ECKO}, PRKO, NR4A1KO and littermate controls were treated with hormones as previously described (Lydon et al., 1995). Details on hormone treatment can be found in Extended Experimental Procedures.

Vascular Permeability Assays

Following hormone treatment, mice were injected i.v. with either Evans blue dye (Miles assay; 1 ml/kg of 3% Evans blue) or select lectins and allowed to circulate for 20 min. before perfusion fixation (1% paraformaldehyde). Select organs were removed, blotted dry, and weighed (wet weight). Evans blue was extracted from tissues with formamide overnight at 55°C and measured in duplicate by a sp ectrometer at 620 nm. Details on extraction and quantification of albumin are in Extended Experimental Procedures.

Embryo Isolation and Implantation

Embryos were obtained from wild-type females mated with fertile males. Embryos (2–4 cell stage) were recovered by flushing uteri with HBSS. 12 embryos were transferred into anesthetized pseudopregnant females via the infundibulum into the ipsilateral ampulla of the uterine tube. The peritoneum was sutured and skin closed with a clamp. Counts of implantation sites were performed using a dissecting microscope (Leica Micosystems, Buffalo Grove, IL) and image acquisition and analytic software (SPOT Imaging Solutions, Sterling Heights, MI).

Immunohistochemistry

Tissue (5μm) and/or vibratome (300μm) sections were immunostained with antibodies against PR (SP2, Lab vision, Kalamazoo, MI), PECAM-1 (MEC 13.1, BD Biosciences, Franklin Lakes, NJ) and GFP (Abcam, Cambridge, MA). Antigen retrieval using Tris-EDTA (pH 9.0) was required for PR staining of formalin embedded tissues. Alexa Fluor secondary antibodies were used to recognize primary antibodies (Molecular Probes, Life Technologies, Grand Island, NY). Sections were analyzed using a Zeiss LSM 510 META multiphoton microscope with built in Axiocam and acquired using Zen software (Zeiss, Germany). Details of β-galactosidase staining can be found in Extended Experimental Procedures.

Immunoblotting and Immunoprecipitation

Proteins were resolved by SDS-PAGE, transferred to nitrocellulose (Optitran BA-S 83; Dassel, Germany), and incubated overnight with antibodies against: PR (SP2, Lab Vision, Kalamazoo, MI), VE-cadherin (Cell Signaling, Danvers, MA), PECAM-1 (Cell Signaling, Danvers, MA), Claudin-5 (Invitrogen; Grand Island, NY), β-catenin (Sigma, St. Louis, MO), β-actin (Sigma, St. Louis, MO), pVE-Cadherin (pY685, (Orsenigo et al., 2012), FAK (BD Bioscience, Franklin Lakes, NJ), β1-integrin (Millipore, AB1952) and and myc (Cell Signaling, Danvers, MA). Blots were incubated with HRP-conjugated secondary (Bio-Rad Laboratories, Hercules, CA), developed with Supersignal West Pico Chemiluminescent Substrate (Thermo Scientific, Kalamazoo, MI) and imaged by a Bio-Rad ChemiDoc XRS+ and accompanying Image Lab software (Bio-Rad Laboratories, Hercules, CA). Cell fractionation experiments were carried out as previously described (Behrmann et al., 2004). Details on immunoprecipitation can be found in Extended Experimental Procedures.

Electrical Cell-Substrate Impedance Sensing

Human umbilical vein endothelial cells, passages 4–6, were cultured in MCDB-131 (VEC Technologies, Rensselaer, NY) with the addition of 10% fetal bovine serum (Omega Scientific, Tarzana, CA) that was stripped using 0.25% dextran coated charcoal (Sigma, St. Louis, MO). PR infected HUVECS were seeded onto 8W10E+ arrays and treated with P4 (100nM) after cells reached confluence (Applied Biophysics, Troy, NY). Data was acquired and analyzed using ECIS software (Applied Biophysics, Troy, NY). Details on reagents used in ECIS experiments see Extended Experimental Procedures.

Chromatin immunoprecipitation and library preparation

For each condition (negative control, PR+P4, PR only, and IgG control) 10×10^6 and 2×10^6 cultured HUVECs were used per IP for ChIP-seq and ChIP-qPCR, respectively. HUVECs were infected with a PR lentivirus, grown to confluence, and then treated with P4 for 1h. The library for sequencing was constructed using Ovation Ultralow IL Multiplex System 1–8 according to manufacturer's instructions (Nugen, San Carlos, CA). Libraries were sequenced using HIseq-2000 (Illumina, San Diego, CA) to obtain 50 bp long reads. ChIP-seq data sets have been deposited in the NCBI Gene Expression Omnibus with the accession number GSE43786. For details on ChIP and how peaks were called and analyzed see Extended Experimental Procedures.

RNA isolation, qPCR, and library preparation

Total RNA was extracted from organs and cells using RNeasy Kit (Qiagen, Valencia, CA), cDNA generated using SuperScript First-strand Synthesis System (Invitrogen, Grand Island, NY) and quantitative real-time PCR was performed using SYBR Green reagent (Qiagen, Valencia, CA) and detected using an Opticon2 PCR machine (MJ Research; BioRad, Hercules, CA). The library for sequencing was constructed using an Illumina Multiplex System according to manufacturer's instructions (Illumina, San Diego, CA). Libraries were

sequenced using HIseq-2000 (Illumina, San Diego, CA) to obtain 50 bp long reads. RNA-seq data sets have been deposited in the NCBI Gene Expression Omnibus with the accession number GSE46502. For details on how differentially expressed genes were identified and analyzed see Extended Experimental Procedures.

Statistical Analysis

For statistical analysis, Student's unpaired two-tailed t-test was used for all comparisons.

Supplementary Material

Refer to Web version on PubMed Central for supplementary material.

Acknowledgments

The authors thank Kari Alitalo for providing the tie1 construct, Liman Zhao for mouse husbandry, and the Tissue Procurement Core Laboratory Shared Resource. The study was supported by funds from RO1HL74455-01 to MLIA; T32HL69766, AHA-11PRE7300043 and Iris Cantor-UCLA Women's Health Center to LMG and Mobilitas Grant MJD284 and Leukemia and Lymphoma Society 5737-13 to TO. The UCLA Vector Core generated lentiviral vectors (supported by JCCC/P30 CA016042 and CURE/P30 DK041301).

References

Arnal JF, Fontaine C, Billon-Galés A, Favre J, Laurell H, Lenfant F, Gourdy P. Estrogen receptors and endothelium. Arterioscler Thromb Vasc Biol. 2010; 30:1506–1512. [PubMed: 20631350]

Atkins GB, Jain MK, Hamik A. Endothelial differentiation: molecular mechanisms of specification and heterogeneity. Arterioscler Thromb Vasc Biol. 2011; 31:1476–1484. [PubMed: 21677290]

Behrmann I, Smyczek T, Heinrich PC, Schmitz-Van de Leur H, Komyod W, Giese B, Müller-Newen G, Haan S, Haan C. Janus kinase (Jak) subcellular localization revisited: the exclusive membrane localization of endogenous Janus kinase 1 by cytokine receptor interaction uncovers the Jak receptor complex to be equivalent to a receptor tyrosine kinase. J Biol Chem. 2004; 279:35486–35493. [PubMed: 15123646]

Bernelot Moens SJ, Schnitzler GR, Nickerson M, Guo H, Ueda K, Lu Q, Aronovitz MJ, Nickerson H, Baur WE, Hansen U, et al. Rapid estrogen receptor signaling is essential for the protective effects of estrogen against vascular injury. Circulation. 2012; 126:1993–2004. [PubMed: 22997253]

Chappell JC, Bautch VL. Vascular development: genetic mechanisms and links to vascular disease. Curr Top Dev Biol. 2010; 90:43–72. [PubMed: 20691847]

Das A, Mantena SR, Kannan A, Evans DB, Bagchi MK, Bagchi IC. De novo synthesis of estrogen in pregnant uterus is critical for stromal decidualization and angiogenesis. Proc Natl Acad Sci USa. 2009; 106:12542–12547. [PubMed: 19620711]

Dejana E, Orsenigo F, Lampugnani MG. The role of adherens junctions and VE-cadherin in the control of vascular permeability. J Cell Sci. 2008; 121:2115–2122. [PubMed: 18565824]

Dvorak HF. Vascular permeability to plasma, plasma proteins, and cells: an update. Curr Opin Hematol. 2010; 17:225–229. [PubMed: 20375889]

Edwards DP, Altmann M, DeMarzo A, Zhang Y, Weigel NL, Beck CA. Progesterone receptor and the mechanism of action of progesterone antagonists. The Journal of Steroid Biochemistry and Molecular Biology. 1995; 53:449–458. [PubMed: 7626494]

Fan X, Krieg S, Kuo CJ, Wiegand SJ, Rabinovitch M, Druzin ML, Brenner RM, Giudice LC, Nayak NR. VEGF blockade inhibits angiogenesis and reepithelialization of endometrium. Faseb J. 2008; 22:3571–3580. [PubMed: 18606863]

Franco HL, Rubel CA, Large MJ, Wetendorf M, Fernandez-Valdivia R, Jeong JW, Spencer TE, Behringer RR, Lydon JP, DeMayo FJ. Epithelial progesterone receptor exhibits pleiotropic roles in uterine development and function. Faseb J. 2012; 26:1218–1227. [PubMed: 22155565]

Gellersen B, Brosens IA, Brosens JJ. Decidualization of the human endometrium: mechanisms, functions, and clinical perspectives. Semin Reprod Med. 2007; 25:445–453. [PubMed: 17960529]

Hickey M, Fraser IS. Surface vascularization and endometrial appearance in women with menorrhagia or using levonorgestrel contraceptive implants. Implications for the mechanisms of breakthrough bleeding. Hum Reprod. 2002; 17:2428–2434. [PubMed: 12202436]

Huang DW, Sherman BT, Lempicki RA. Bioinformatics enrichment tools: paths toward the comprehensive functional analysis of large gene lists. Nucleic Acids Res. 2009; 37:1–13. [PubMed: 19033363]

Hyder SM, Stancel GM, Chiappetta C, Murthy L, Boettger-Tong HL, Makela S. Uterine expression of vascular endothelial growth factor is increased by estradiol and tamoxifen. Cancer Res. 1996; 56:3954–3960. [PubMed: 8752163]

Iafrati MD, Karas RH, Aronovitz M, Kim S, Sullivan TR, Lubahn DB, O'Donnell TF, Korach KS, Mendelsohn ME. Estrogen inhibits the vascular injury response in estrogen receptor alpha-deficient mice. Nat Med. 1997; 3:545–548. [PubMed: 9142124]

Ismail PM, Li J, DeMayo FJ, O'Malley BW, Lydon JP. A novel LacZ reporter mouse reveals complex regulation of the progesterone receptor promoter during mammary gland development. Molecular Endocrinology. 2002; 16:2475–2489. [PubMed: 12403837]

Strauss, JF.; Barbieri, RL. Yen and Jaffe's Reproductive Endocrinology. Elsevier Health Sciences; 2009.

Kim KH, Bender JR. Membrane-initiated actions of estrogen on the endothelium. Mol Cell Endocrinol. 2009; 308:3–8. [PubMed: 19549586]

Komarova Y, Malik AB. Regulation of endothelial permeability via paracellular and transcellular transport pathways. Annu Rev Physiol. 2010; 72:463–493. [PubMed: 20148685]

Kovacs G. Progestogen-only pills and bleeding disturbances. Hum Reprod. 1996; 11(Suppl 2):20–23. [PubMed: 8982741]

Krikun G, Schatz F, Taylor R, Critchley HOD, Rogers PAW, Huang J, Lockwood CJ. Endometrial endothelial cell steroid receptor expression and steroid effects on gene expression. Journal of Clinical Endocrinology & Metabolism. 2005; 90:1812–1818. [PubMed: 15613410]

Large MJ, DeMayo FJ. The regulation of embryo implantation and endometrial decidualization by progesterone receptor signaling. Mol Cell Endocrinol. 2012; 358:155–165. [PubMed: 21821095]

Lydon JP, DeMayo FJ, Conneely OM, O'Malley BW. Reproductive phenotpes of the progesterone receptor null mutant mouse. The Journal of Steroid Biochemistry and Molecular Biology. 1996; 56:67–77. [PubMed: 8603049]

Lydon JP, DeMayo FJ, Funk CR, Mani SK, Hughes AR, Montgomery CA, Shyamala G, Conneely OM, O'Malley BW. Mice lacking progesterone receptor exhibit pleiotropic reproductive abnormalities. Genes Dev. 1995; 9:2266–2278. [PubMed: 7557380]

Maybin JA, Duncan WC. The human corpus luteum: which cells have progesterone receptors? Reproduction. 2004; 128:423–431. [PubMed: 15454637]

McKenna NJ, O'Malley BW. From ligand to response: generating diversity in nuclear receptor coregulator function. The Journal of Steroid Biochemistry and Molecular Biology. 2000; 74:351–356. [PubMed: 11162944]

Orsenigo F, Giampietro C, Ferrari A, Corada M, Galaup A, Sigismund S, Ristagno G, Maddaluno L, Koh GY, Franco D, et al. Phosphorylation of VE-cadherin is modulated by haemodynamic forces and contributes to the regulation of vascular permeability in vivo. Nat Commun. 2012; 3:1208. [PubMed: 23169049]

Pearen MA, Muscat GEO. Minireview: Nuclear hormone receptor 4A signaling: implications for metabolic disease. Mol Endocrinol. 2010; 24:1891–1903. [PubMed: 20392876]

Pei L, Castrillo A, Tontonoz P. Regulation of macrophage inflammatory gene expression by the orphan nuclear receptor Nur77. Molecular Endocrinology. 2006; 20:786–794. [PubMed: 16339277]

Perrot-Applanat M, Cohen-Solal K, Milgrom E, Finet M. Progesterone receptor expression in human saphenous veins. Circulation. 1995; 92:2975–2983. [PubMed: 7586268]

Regan ER, Aird WC. Dynamical systems approach to endothelial heterogeneity. Circ Res. 2012; 111:110–130. [PubMed: 22723222]

Rubel CA, Lanz RB, Kommagani R, Franco HL, Lydon JP, DeMayo FJ. Research Resource: Genome-Wide Profiling of Progesterone Receptor Binding in the Mouse Uterus. Molecular Endocrinology. 2012

Runic R, Schatz F, Wan L, Demopoulos R, Krikun G, Lockwood CJ. Effects of norplant on endometrial tissue factor expression and blood vessel structure. Journal of Clinical Endocrinology & Metabolism. 2000; 85:3853–3859. [PubMed: 11061549]

Shifren JL, Tseng JF, Zaloudek CJ, Ryan IP, Meng YG, Ferrara N, Jaffe RB, Taylor RN. Ovarian steroid regulation of vascular endothelial growth factor in the human endometrium: implications for angiogenesis during the menstrual cycle and in the pathogenesis of endometriosis. Journal of Clinical Endocrinology & Metabolism. 1996; 81:3112–3118. [PubMed: 8768883]

Shoupe D, Mishell DR, Bopp BL, Fielding M. The significance of bleeding patterns in Norplant implant users. Obstet Gynecol. 1991; 77:256–260. [PubMed: 1899135]

Sugino N, Kashida S, Karube-Harada A, Takiguchi S, Kato H. Expression of vascular endothelial growth factor (VEGF) and its receptors in human endometrium throughout the menstrual cycle and in early pregnancy. Reproduction. 2002; 123:379–387. [PubMed: 11882015]

Vázquez F, Rodríguez-Manzaneque JC, Lydon JP, Edwards DP, O'Malley BW, Iruela-Arispe ML. Progesterone regulates proliferation of endothelial cells. J Biol Chem. 1999; 274:2185–2192. [PubMed: 9890981]

Wetendorf M, DeMayo FJ. The progesterone receptor regulates implantation, decidualization, and glandular development via a complex paracrine signaling network. Mol Cell Endocrinol. 2012; 357:108–118. [PubMed: 22115959]

Zhao D, Qin L, Bourbon PM, James L, Dvorak HF, Zeng H. Orphan nuclear transcription factor TR3/Nur77 regulates microvessel permeability by targeting endothelial nitric oxide synthase and destabilizing endothelial junctions. Proc Natl Acad Sci USa. 2011; 108:12066–12071. [PubMed: 21730126]

Zhao Y, Bruemmer D. NR4A orphan nuclear receptors: transcriptional regulators of gene expression in metabolism and vascular biology. Arterioscler Thromb Vasc Biol. 2010; 30:1535–1541. [PubMed: 20631354]

Zhu Y, Bian Z, Lu P, Karas RH, Bao L, Cox D, Hodgin J, Shaul PW, Thoren P, Smithies O, et al. Abnormal vascular function and hypertension in mice deficient in estrogen receptor beta. Science. 2002; 295:505–508. [PubMed: 11799247]

Highlights

- Endothelial PR mediates local vascular permeability in response to progesterone
- Restricted expression of PR ensures organ and vessel selectivity to progesterone
- PR activation of NR4A1 (Nur77/TR3) triggers barrier instability in the endothelium

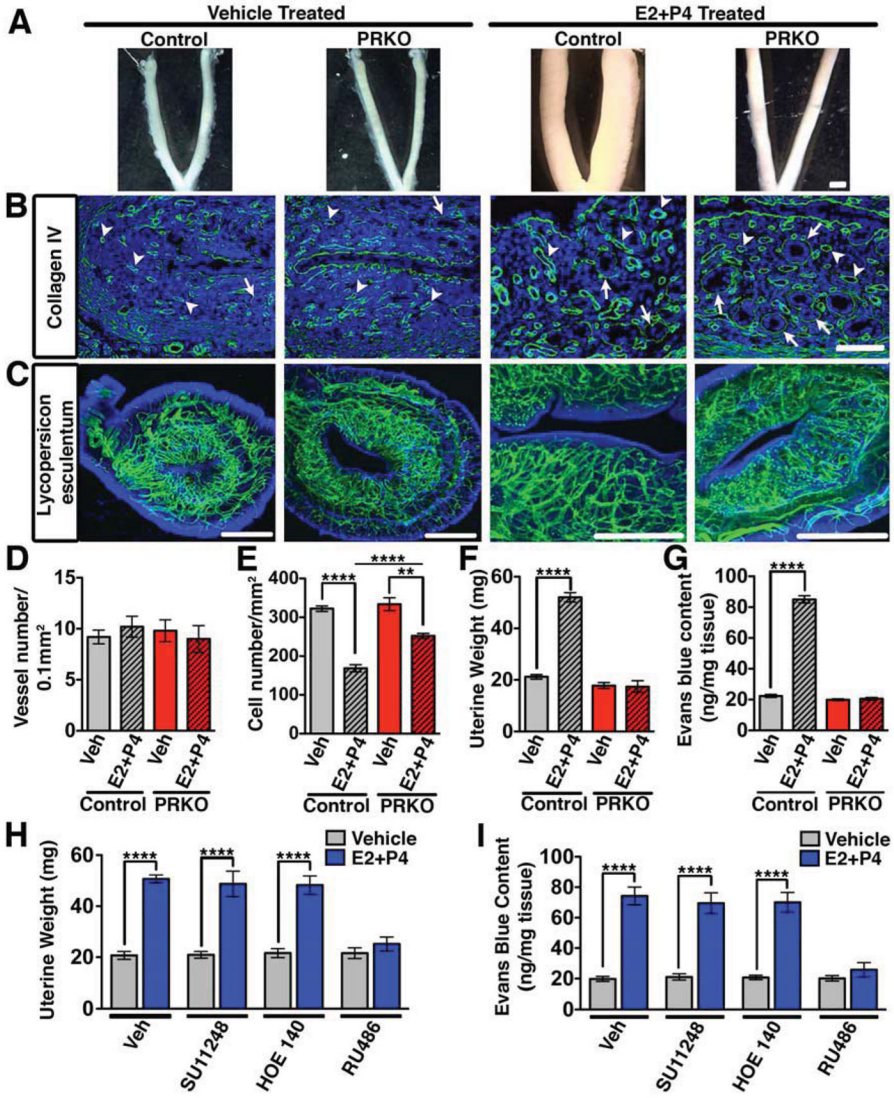

Figure 1. Reduced physiological permeability in the uterus following global PR deletion

(A) Effect of hormones (E2+P4) on control (wild-type) and PRKO uteri. Scale, 3mm. **(B)** Collagen IV immunostaining (green) detects basement membrane of glands (arrows) and blood vessels (arrowheads). Scale, 100μm. **(C)** Uteri following intravascular perfusion with FITC conjugated *Lycopersicum esculentum* lectin. Scale, 1mm. **(D)** Vessel number/0.1mm^2 in control and PRKO mice. **(E)** Uterine cell density/mm^2 in control and PRKO mice. **(F)** Uterine wet weight in control and PRKO mice. **(G)** Uterine Evans blue content measured by the Miles assay. **(H)** Uterine wet weight following concurrent treatment of E2+P4 with inhibitors of VEGFR2 (SU11248), bradykinin (HOE140), and PR (RU486). **(I)** Quantification of Evans blue after the conditions listed in (H). In all panels, error bars = +/−. **p<0.01, ****p<0.0001. n=3–5. See also Figure S1 and Table S1.

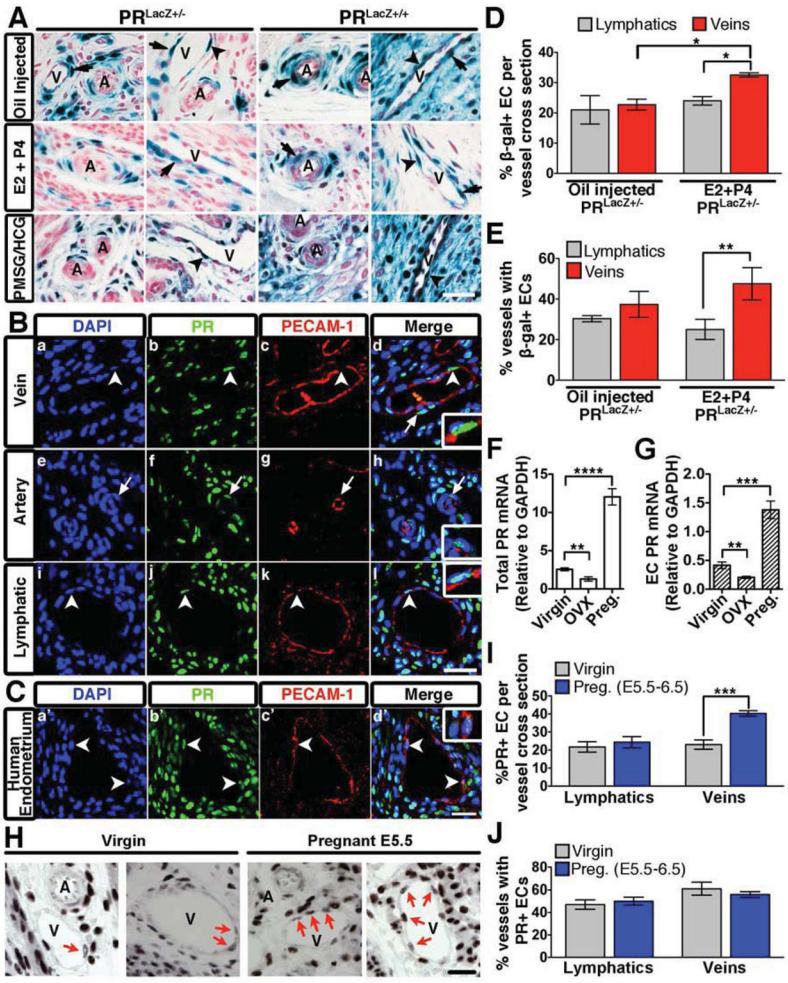

Figure 2. PR expression in the murine vasculature

(A) β-gal positivity in transverse uterine sections from $PR^{LacZ+/-}$ and $PR^{LacZ+/+}$ mice treated with oil, E2 and P4, or PMSG/HCG. Endothelial cells (arrowheads); smooth muscle cells (arrows); veins, V; arteries, A. Nuclear Fast Red was used as a counterstain. **(B,C)** Immunofluorescence of murine (B) and human (C) uterine sections stained for PECAM-1 (red) and PR (green). Nuclei were visualized using DAPI (blue). Endothelial cells (arrowheads); smooth muscle cells (arrows). Insets are higher mag images of PR positive endothelial cells. **(D)** Percentage of β-gal+ endothelial cells per vessel cross-section from $PR^{LacZ+/-}$ mice. n=3. **(E)** Percentage of vessels in the uterus that contain at least one β-gal+ endothelial cell per cross-section. n=3. **(F)** Total PR mRNA levels in the uterus from virgin, ovarectomized (OVX), and pregnant (E5.5) mice. (**G)** PR mRNA levels from isolated uterine endothelial cells from the same mice listed in (F). **(H)** PR protein expression in the endothelium of virgin and pregnant (E5.5) mice. PR+ endothelial cells (arrows); veins, V; arteries, A. **(I)** Percentage of PR+ endothelial cells per vessel cross-section from virgin and pregnant uteri (E5.5). n=3. **(J)** Percentage of vessels from virgin and pregnant uteri that contain at least one PR+ endothelial cell per cross-section. n=3. In all panels, error bars=+/−SEM. Scale=25 μm. *p<0.05, **p<0.01, ***p<0.001 ****p<0.0001. See also Figure S2.

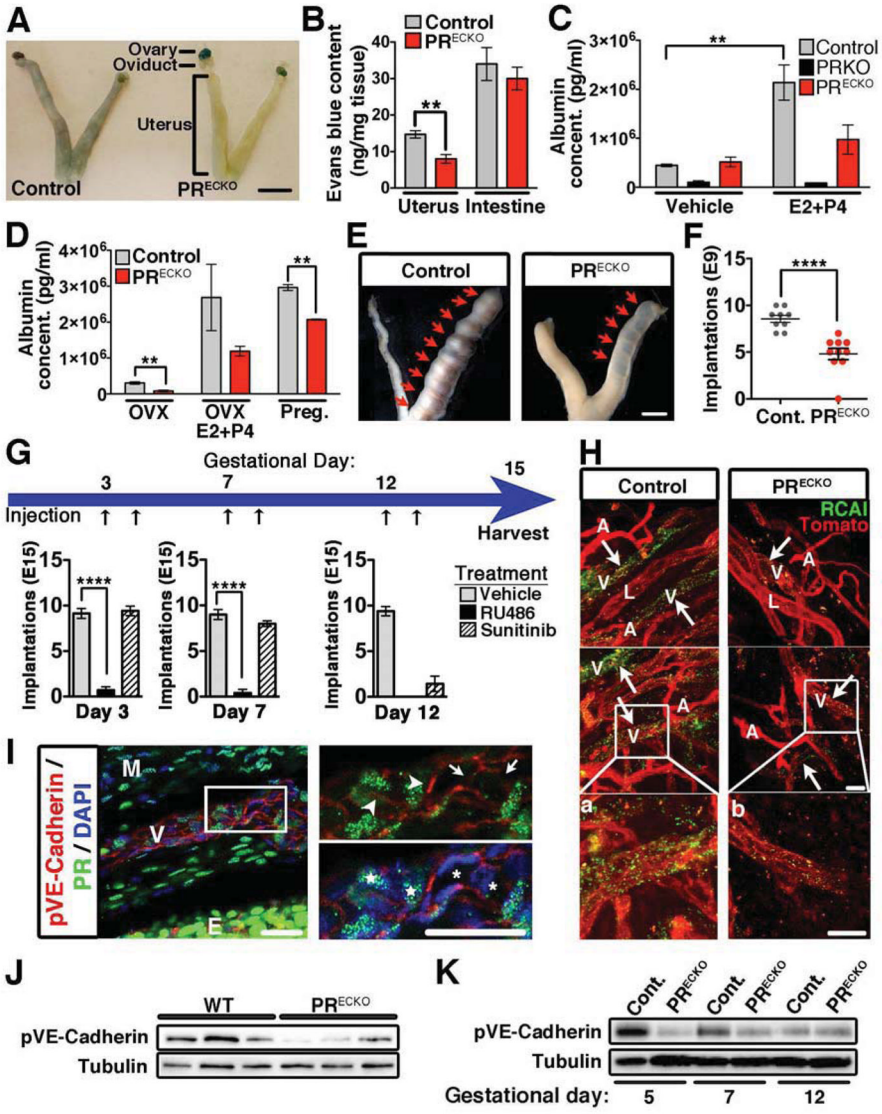

Figure 3. Reduced vascular permeability upon conditional deletion of PR in the endothelial compartment

(A) Evans Blue extravasation in control (PRCE; Cre negative) and PR^{ECKO} mice. Scale, 7mm **(B)** Evans blue content in uterus and intestine following hormone stimulation. n=7–8 **(C)** Uterine albumin concentrations from control, PRKO, and PR^{ECKO} animals following vehicle or E2+P4 treatment. **(D)** Uterine albumin concentrations from ovarectomized (OVX) control and PR^{ECKO} animals following vehicle and E2+P4. Early pregnancy, (gestational day 3), was also examined. **(E)** Whole mount images depicting implantation sites (arrows) in control and PR^{ECKO} mice following embryo transfer. Scale, 5mm. **(F)** Quantification of implantation sites at gestational day 9 following embryo transfer in control and PR^{ECKO} mice. **(G)** Schematic depicting treatment of pregnant control females (gestational days 3, 7, and 12) with vehicle, RU486 (PR antagonist) and Sunitinib (VEGFR2 antagonist). Black arrows represent time of injection. Implantation sites were quantified at E15 and are represented in the bar graphs below. **(H)** *Ricinus communis agglutinin I* (green) and *Lycopersicon esculentum* (red) staining of uteri from control and PR^{ECKO} animals following E2+P4. Arrows indicate sites of permeability (green). artery, A; vein, V; lymphatic, L. **(a,b)** Enlarged images of boxes in (H). Scale, 50μm. **(I)** Immunohistochemistry of pVE-Cadherin

(red) and PR (green). DAPI (blue) shows nuclei. Higher mag in box on right. pVE-Cadherin expression (arrowheads); lack of pVE-Cadherin (arrows); PR+ cell, star; PR− cell, asterisk; myometrium, M; endometrium, E. Scale, 20μm **(J)** Western blot for pVE-Cadherin protein levels in uteri of virgin control and PR^{ECKO} mice. Tubulin=loading control. **(K)** Western blot for total pVE-Cadherin protein levels from pregnant uteri (gestational days 5, 7 and 12) of control and PR^{ECKO} mice. Tubulin=loading control. In all panels, error bars=+/−SEM. **p<0.01, ****p<0.0001. See also Figure S3.

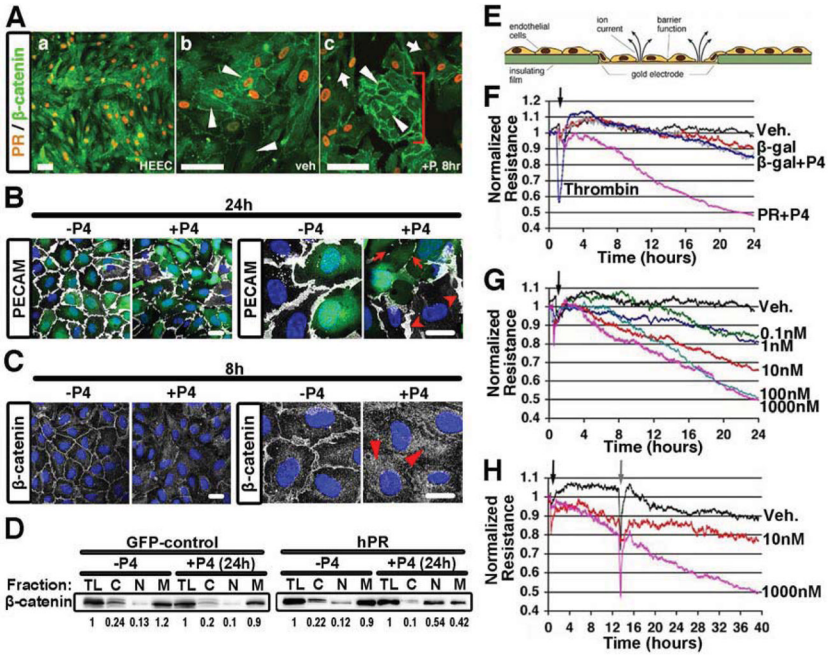

Figure 4. PR activation in endothelial cells results in barrier disruption

(A) Immunohistochemistry of HEEC for PR (orange) and β-catenin (green, arrows). (a) low magnification; (b) high-mag treated with vehicle and (c) high-mag treated with P4. PR-negative cell islands are indicated by the bracket. Scale, 100μm. **(B)** PECAM (white) in HUVECs infected with a PR lentivirus (GFP, green) following 24h of P4 treatment (100nM). DAPI (blue) shows nuclei. Arrows indicate junctional disruption. Arrowheads show presence of PECAM in PR− cells. Scale, 10μm. **(C)** β-catenin (white) in HUVECs infected with a PR lentivirus (green, GFP) following 8h of P4 treatment (100nM). DAPI (blue) shows nuclei. Arrowheads show translocation of β-catenin from the cell membrane to cytosol. Scale, 10μm. **(D)** Presence of β-catenin in subcellular fractions from HUVECs infected with GFP-control or hPR lentivirus. Cells were treated with or without P4 for 24h as indicated. total lysate, TL; cytosol, C; nuclear, N; membrane, M. Numbers below indicate quantification of Western blot. **(E)** Diagram depicting electrical cell-substrate impedance sensing (ECIS). **(F)** Monolayer resistance of HDECs following infection with a PR adenovirus and β-gal control construct. Thrombin used as positive control. **(G)** HDEC monolayer resistance following treatment with increasing concentrations of P4 as indicated. **(H)** Evaluation of HDEC monolayer resistance after removal of P4 from the media. P4 addition (black arrow); P4 removal (grey arrow). n=3–5. See also Figure S4.

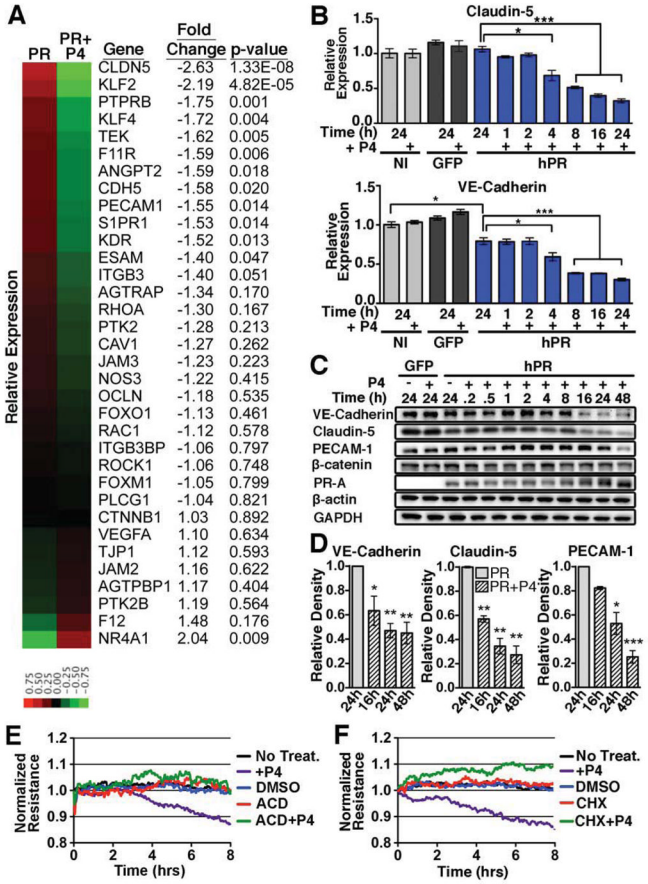

Figure 5. PR activation leads to changes in expression of junctional proteins

(A) Heat map representing the relative expression and fold change of genes known to regulate vascular permeability in PR vs. PR+P4 HUVECS at 4h. **(B)** qPCR of VE-cadherin (*CDH5*) and claudin-5 (*CLDN5*) expression following P4 treatment of non-infected (NI), GFP infected (GFP) and PR infected (hPR) HUVECs. n=3. GFP infected HUVECs were used as a control for infection. **(C)** Western blot analysis of total protein levels from GFP control or PR infected HUVECs following P4 treatment. GAPDH/β-actin=loading controls. Blots are representative of three independent experiments. **(D)** Densitometry of VE-cadherin, claudin-5, and PECAM-1 protein levels following P4 treatment. n=3. **(E,F)** Evaluation of HUVEC monolayer resistance following treatment with cycloheximide (CHX, 10μg/ml), actinomycin D (ACD, 10μg/ml), or P4 and vehicle as indicated. Error bars=+/− SEM. *p<0.05, **p<0.01, ***p<0.001. See also Figure S5.

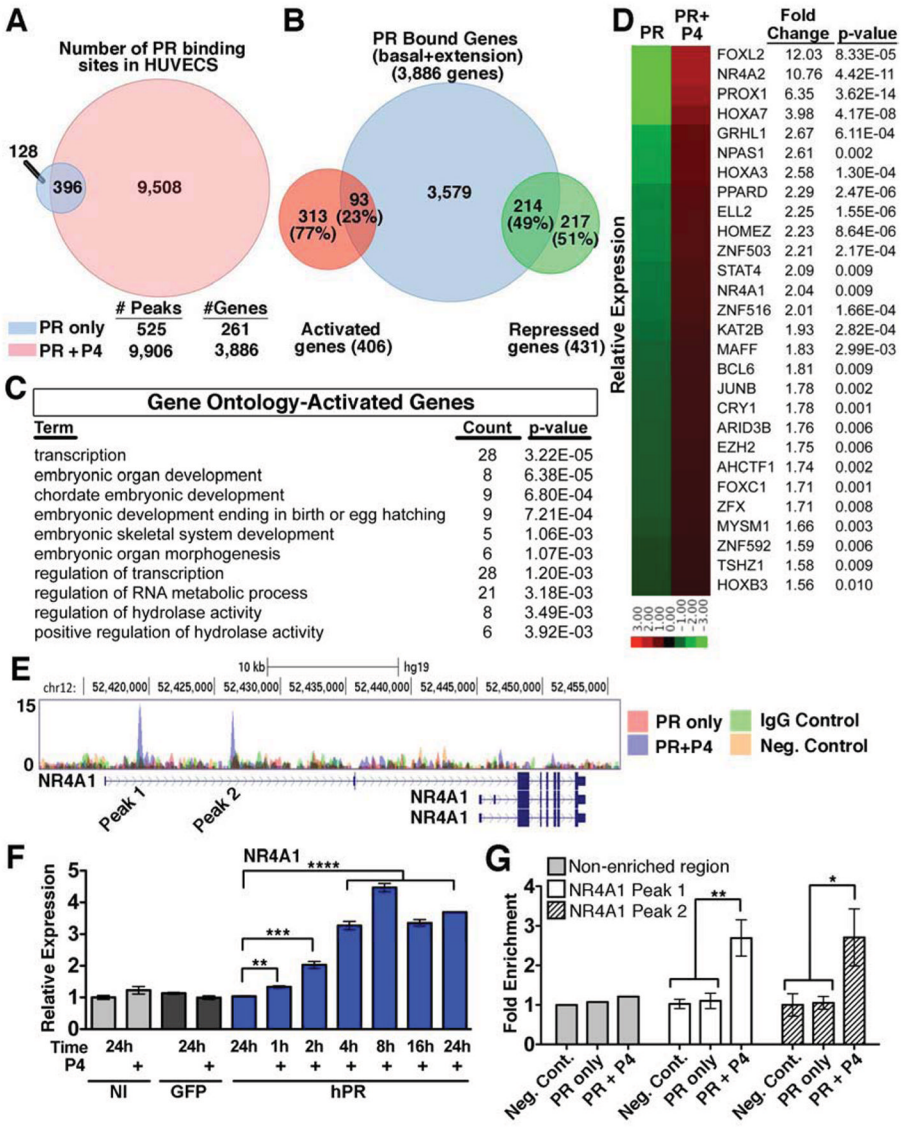

Figure 6. NR4A1 is a direct target of PR

(A) Venn diagram of PR binding peaks between HUVECs treated with (red) or without (blue) P4 for 1h. Predicted gene numbers based on analysis of binding peaks within 50kb of the transcriptional start site. **(B)** Venn Diagram representing the overlap between genes predicted to be regulated by PR by ChIP-seq and genes with a p value less than 0.01 as determined by RNA-seq. **(C)** Top gene ontology terms from activated genes bound by PR as predicted by DAVID. **(D)** Heat map depicting expression and fold change of the 28 transcription factors that were in the top gene ontology pathway from (C). **(E)** Depiction of two PR binding peaks upstream of the NR4A1 gene in the presence of P4. Neg. control=NI HUVECs. **(F)** qPCR analysis of NR4A1 expression following P4 treatment of non-infected (NI), GFP infected (GFP) and PR infected (hPR). n=3. **(G)** ChIP-qPCR analysis of both NR4A1 binding peaks following P4 treatment. *p<0.05, **p<0.01, ***p<0.001, ****p<0.0001. In all panels, error bars=+/− SEM. See also Figure S6 and Table S2.

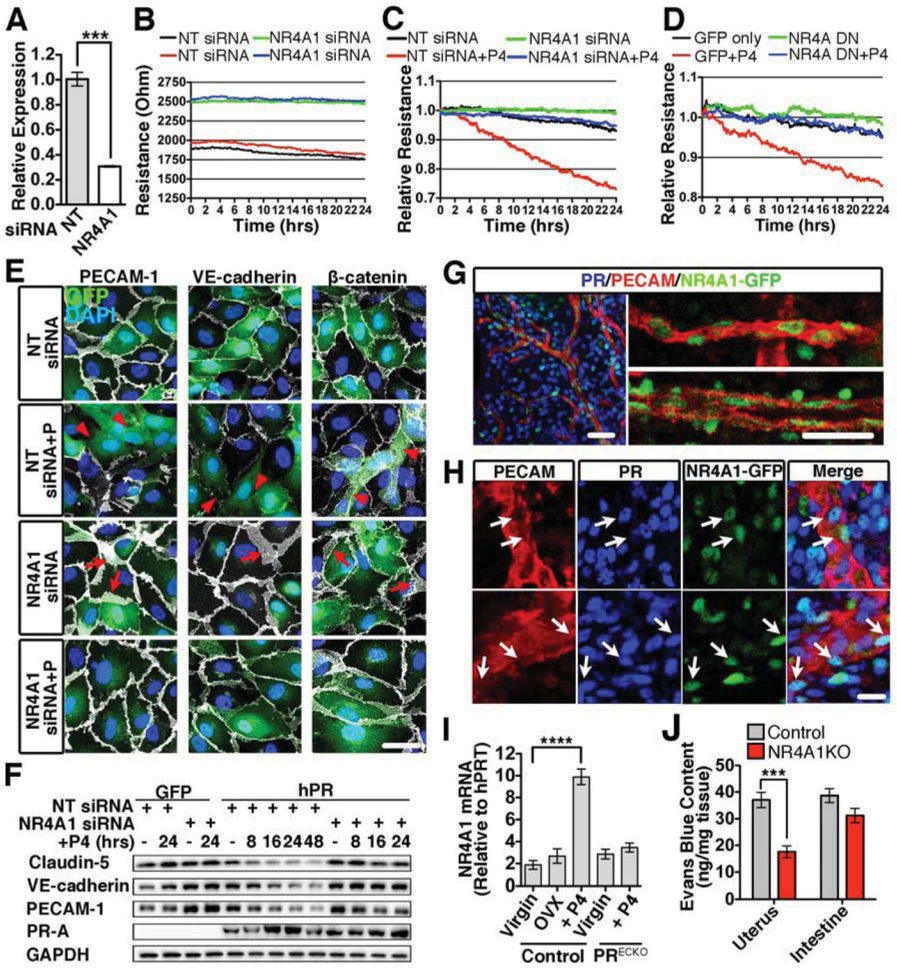

Figure 7. Knockdown of NR4A1 inhibits progesterone-mediated permeability

(A) qPCR analysis of NR4A1 following transfection of HUVECs with either non-targeting (NT) or NR4A1 siRNA. n=3. **(B)** Baseline HUVEC monolayer resistance following NR4A1 knockdown. **(C)** HUVEC monolayer resistance after transfection with NR4A1 or NT siRNA in the presence of P4. **(D)** HUVEC monolayer resistance following adenoviral infection with a NR4A family dominant negative (NR4A DN) and control (GFP) in the presence of P4. **(E)** HUVECs expressing PR (GFP, green) and transfected with either NT or NR4A1 siRNA were treated with P4 for 24h. PECAM, VE-cadherin, and β–catenin (white) were used to visualize junctions. DAPI (blue) denotes nuclei. Arrowheads indicate a reduction in junctional proteins. Arrows show expanded junctional area. Scale, 50μm. **(F)** Junctional proteins from GFP or PR infected HUVECs following transfection with either NT or NR4A1 siRNA followed by P4 treatment. GAPDH=loading control. **(G)** NR4A1 (GFP, green) localization in the vascular endothelium in vivo (PECAM, red). Scale, 25μm **(H)** PR (blue) and NR4A1 (GFP, green) colocalization in uterine vasculature (PECAM, red). Arrows indicate endothelial cells with NR4A1 and PR. Scale, 20μm **(I)** qPCR of NR4A1 from the uteri of virgin, ovarectomized (OVX) and PR^{ECKO} mice treated with or without P4. n=3. **(J)** Evans blue content from the uterus and intestine following hormone stimulation of control (wild-type) and NR4A1KO mice. ***p<0.001, ****p<0.001. Error bars=+/− SEM. See also Figure S7.